Physical and Perceptual Evaluation of Electric Guitar Loudspeakers

Wolfgang Klippel

KLIPPEL GmbH, 01309 Dresden, E-Mail:wklippel@klippel.de

Introduction

Loudspeakers used in combination with electric guitars shall not reproduce the electric signal captured by the pickup with low signal distortion but the loudspeaker is part of the musical instrument and is allowed to shape the spectral components of the sound and to create new signal components as well [1]. This paper presents a systematic methodology to investigate the influence of the loudspeaker of the reproduction of typical guitar sounds. A combination of measurement, signal analysis, physical modeling and listening test reveals the critical modal resonances, dominant nonlinearities and other causes which generated the characteristic sound. This knowledge is required to optimize the design of the passive loudspeaker and to develop software algorithms that synthesize those distortion generating a desired artistic effect. This analysis is illustrated on a transducer used in many guitar loudspeakers.

Signal Distortion

Figure 1 shows a black box model that explains the generation of additional distortion components in the output signal $p(t)$ which are not in the input signal $u(t)$.
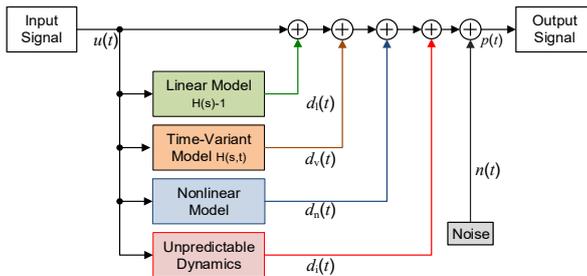

Figure 1: Black box modeling of the distortion components generated in a loudspeaker.

The linear subsystem with the transfer function $H(s)$-1 in

Figure 1 generates the linear distortion component $p_l(t)$ which represents the time-invariant deviation of the output signal from the input signal at small amplitudes. Those linear distortion $d_l(t)$ can be predicted by equivalent circuits and numerical simulation (FEA, BEA) using lumped parameters (TS), modal parameters and geometry and material information.

The time-variant subsystem in

Figure 1 generates a distortion signal that is coherent with the stimulus but varies over time. The heating of the coil increases the voice coil resistance. In consequence, the output at the resonance frequency is boosted due to the lower electrical damping but reduces the output at all other frequencies. The visco-elastic behavior, aging and fatigue of the suspension material also contributes to this kind of distortion.

The nonlinear system in

Figure 1 generates the nonlinear distortion signal $d_n(t)$ that represents the regular nonlinearities in the loudspeaker system which are related to the geometry, material and other design criteria. This distortion signal $d_n(t)$ is incoherent with the stimulus signal but has deterministic properties, which can be revealed by repeating the measurement. This signal becomes negligible in guitar loudspeakers, if the amplitude of stimulus is sufficiently small.

The last subsystem in

Figure 1 represents signal distortion $d_i(t)$ which are not related to the design goals but are related to unpredictable nonlinear dynamics caused by loudspeaker defects. Those distortions are also incoherent with the stimulus but they have usually much less energy than the regular nonlinear distortion $d_n(t)$ and can also not be modelled due to the random nature of most defects. A unique characteristic is a much higher crest factor than for regular nonlinear distortion. The impulsive distortions reflect as high frequency components in the reproduced audio signal spectrum. They are easily audible for a low frequency stimulus and degrade the sound quality significantly.

While the linear and nonlinear distortion generated by the first three subsystems are exploited and intentionally generated in guitar loudspeakers, the irregular distortion $d_i(t)$ indicate a defective speaker that has to be replaced before the distortion become audible.

In-Situ Testing in Target Application

The systematic evaluation of a loudspeaker from a physical and perceptual perspective while reproducing typical guitar sounds requires a recording and differential auralization techniques to separate the distortion components by linear or nonlinear modeling [2].
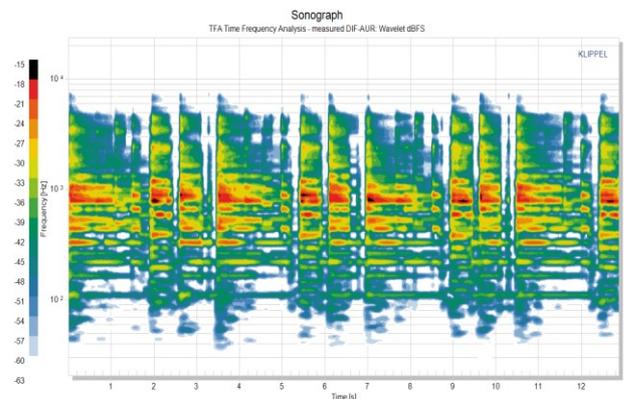

Figure 2: Sound pressure level versus frequency and time (sonograph) of the reproduced guitar sound stimulus.

Figure 2 shows the spectrum of a typical guitar sound stimulus of 13 s with a maximum in sound pressure at 1 kHz and low spectral energy below 150 Hz. Figure 3 shows the internal

states of the guitar loudspeaker while recording this stimulus. The maximum real input power averaged over 1s exceeds 20 W while the high crest factor of the stimulus generates a peak voltage at the terminals at 60 V. The loudspeaker generates a significantly higher positive excursion (4 mm) than negative excursion (3 mm): This indicates asymmetrical nonlinearities inherent in the transducer rectifying the AC signal and generating a DC displacement, dynamically. The voice coil resistance varies by more than 15 %, indicating a significant increase of voice coil temperature.
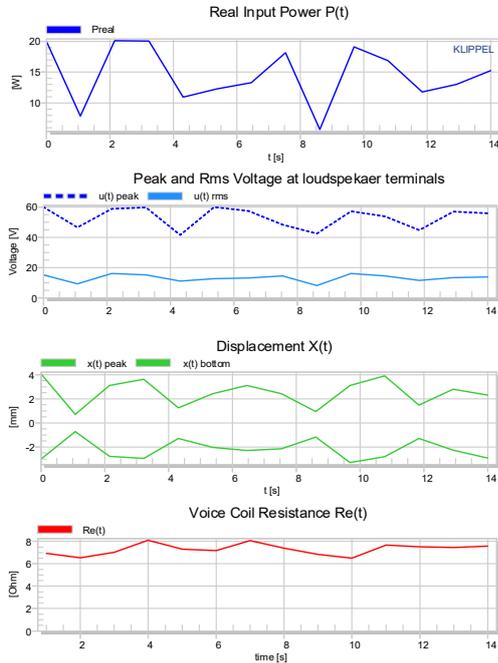

Figure 3: Real input power, peak and rms voltage, peak and bottom displacement and the variation of the voice coil resistance versus time.
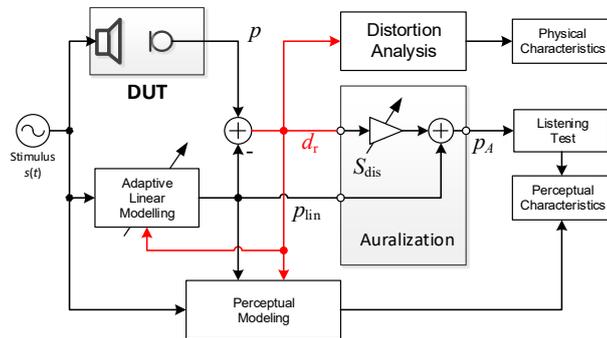

Figure 4: Evaluation of the loudspeaker while using typical guitar sound from the pickup as a stimulus.

A simple technique is shown in Figure 4 where a linear residuum $d_r(t)$ is generated by adaptive linear modeling of the transfer path from the speaker terminals to the microphone output and subtracting the modeled signal $p_{lin}(t)$ from the measured sound pressure $p(t)$. The linear model is adaptively adjusted to the device under test by minimizing the residuum $d_r(t)$. It compensates also for any time-varying linear transducer properties but cannot explain any distortion components that are incoherent to the electrical stimulus $s(t)$. The particular guitar loudspeaker under test generates 1-2 dB variation of the amplitude response within a few seconds due

to voice coil heating. Perceptual modeling can be used to calculate the loudness spectra of the electric stimulus $s(t)$ and modeled linear signal $p_{lin}(t)$ to describe the variation of sharpness, roughness, coloration and other perceptual characteristics.
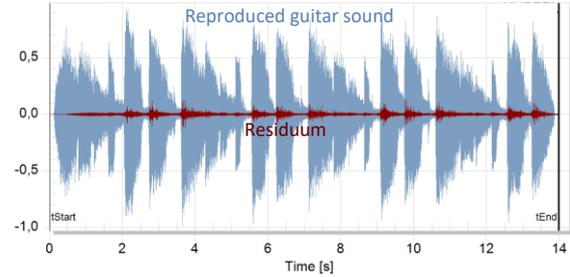

Figure 5: Nonlinear distortion (residuum $d_r(t)$) separated from the reproduced guitar sound stimulus $p(t)$.

More important is the residuum $d_r(t)$ which contains the regular nonlinear and irregular distortion generated by loudspeaker nonlinearities and defects. Careful listening to the residuum $d_r(t)$ of the example guitar loudspeaker does not reveal any indication for impulsive distortion caused by voice coil rubbing or bottoming, parasitic vibration of loose parts and other defects. However, the residuum $d_r(t)$ contains significant nonlinear distortion at low frequencies, generated when the stimulus $s(t)$ contains a significant bass signal.
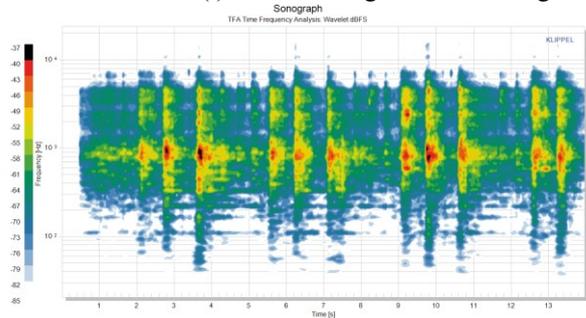

Figure 6: Sonograph showing the nonlinear distortion (residuum) in the reproduced guitar sound stimulus versus time and frequency.

Auralization of Signal Distortion

Mixing the modeled signal $p_{lin}(t)$ and the weighted residuum $S_{dis} \cdot d_r(t)$ allows to generate virtual loudspeaker outputs where the distortion is attenuated or enhanced by scaling factor S_{dis} [5]. The audibility, preference and suitability for the artistic expression can be evaluated by performing a double-blind listening test. The nonlinear distortion generated in the particular loudspeaker have to be increased by S_{dis} = 12 dB in order to make them audible. The spectral components of the nonlinear distortion shown as a sonograph in Figure 6 versus time and frequency are about 20 dB lower than the linear components and are almost masked by the dense spectrum of the particular guitar sample shown in Figure 2. Furthermore, the nonlinear distortions are also coupled to the musical time structure and are not recognized as an independent event disturbing the musical idea. The nonlinearities in the loudspeaker increase the dynamics of the reproduced guitar sound, which corresponds to higher crest factor measured in the residuum $d_r(t)$. The nonlinear distortion becomes more audible if a less complex guitar stimulus (e.g. single tone) is

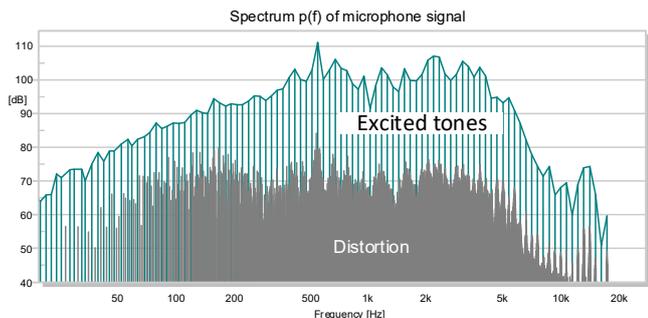played or equalization is applied to enhance the low frequency components below 150 Hz.

Figure 7: Sound pressure spectrum of a reproduced multi-tone stimulus at 25 V total terminal voltage.

Nonlinear Distortion Measurement

Figure 8 shows the sound pressure spectrum of a reproduced sparse multi-tone complex comprising 10 tones per octave over the full audio band where all the tones have the same voltage amplitude [3]. The harmonic and intermodulation distortion show between the excited frequencies at almost the same level between 50 Hz and 5 kHz. The fundamental components that are rising in this frequency band are about 10 to 25 dB higher.
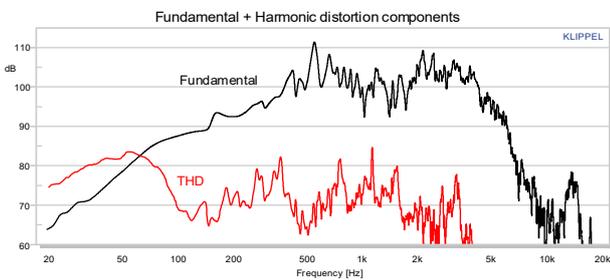

Figure 8: Total harmonic distortion (THD) compared to the fundamental component in SPL generated by a sinusoidal sweep with 25 V_{RMS} at the input terminals.

Figure 8 shows the total harmonic distortion (*THD*) generated by a single tone of 25 V_{RMS}. This signal generates higher voice coil displacement and the *THD* components exceed the fundamental component at low frequencies. At higher frequencies there are peaks at distinct frequencies.
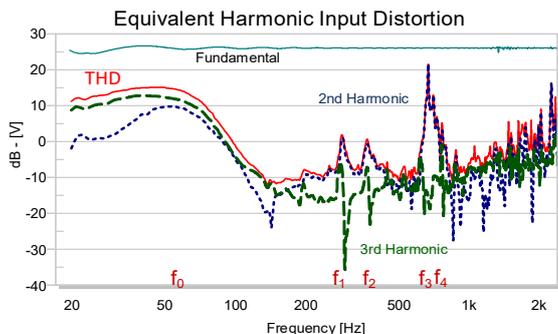

Figure 9: 2nd-order, 3rd-order components and total harmonic distortion compared to the fundamental component transformed to the loudspeaker input terminals

The interpretation of the harmonic distortion can be simplified by filtering the sound pressure signal with the inverse linear transfer function of the speaker, which effectively transforms all signal components to the loudspeaker input terminals [5**Fehler! Verweisquelle konnte nicht gefunden werden.Fehler! Verweisquelle konnte nicht gefunden werden.Fehler! Verweisquelle konnte nicht gefunden werden.Fehler! Verweisquelle konnte nicht gefunden werden.**]. The fundamental component becomes an almost constant value corresponding to the amplitude of 25 V_{RMS} of the sinusoidal sweep and the nonlinear compression effect. The harmonic distortions appear as equivalent input distortion (*EHID* **Fehler! Verweisquelle konnte nicht gefunden werden.**]) in Volt and can directly be compared to the excitation voltage. The frequency responses of *EHID* are relatively smooth curves and shows the distortions close the output of the nonlinear system without the linear transfer path through the mechanical and acoustical system generating a complex frequency response with additional peaks and dips as shown in Figure 8. The total value of the *EHID* at the resonance frequency f_0 of the fundamental piston mode is 15 dB below the input voltage level. At higher frequencies f_1, f_2, f_3 there are distinct peak values in the 2nd-order distortion in *EHID*.
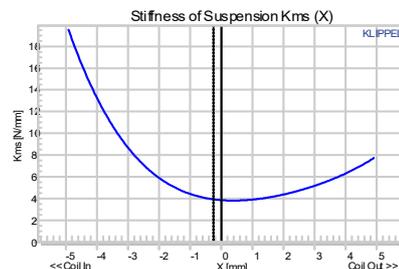

Figure 10: Stiffness $K_{ms}(x)$ versus displacement x.

Dominant Loudspeaker Nonlinearities

Nonlinear system identification can be used to measure the dominant nonlinearities inherent in the guitar loudspeaker **Fehler! Verweisquelle konnte nicht gefunden werden.**7].

Figure 10 reveals a significant asymmetry in the measured stiffness $K_{ms}(x)$ versus displacement x that generates significant 2nd-order harmonics at the fundamental resonance frequency f_0 as shown in Figure 8.
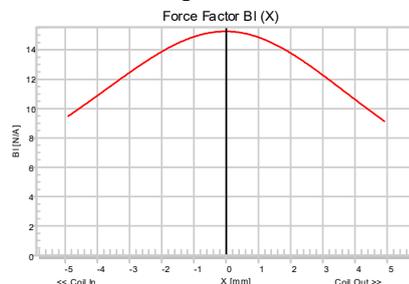

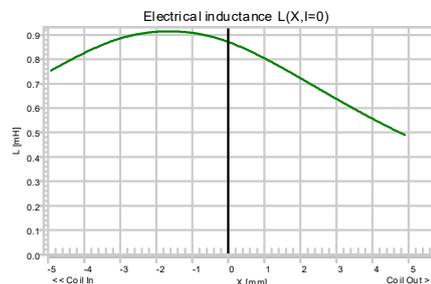
Figure 11: Force factor $Bl(x)$ versus displacement x.

Figure 12: Voice coil inductance $L(x)$ versus displacement x.

Figure 11 shows an almost perfect symmetrical characteristic of the force factor nonlinearity $Bl(x)$ that generates 3rd-order harmonic distortion for a single tone with a frequency below 100 Hz in Figure 8 and causes amplitude intermodulation of any signal reproduced by the guitar speaker.

The nonlinear dependency of the voice coil inductance $L(x)$ on displacement x as shown in Figure 12 also generates significant intermodulation distortion in the audio band. The intermodulation distortion generated by $Bl(x)$ and $L(x)$ are dominant in the multi-tone distortion measurement and in the residuum of the reproduced guitar sound stimulus. Since the high-frequency components are modulated by a low frequency bass signal ($f < 100$ Hz) the variation of the envelope is perceived as an increased roughness by the human ear.
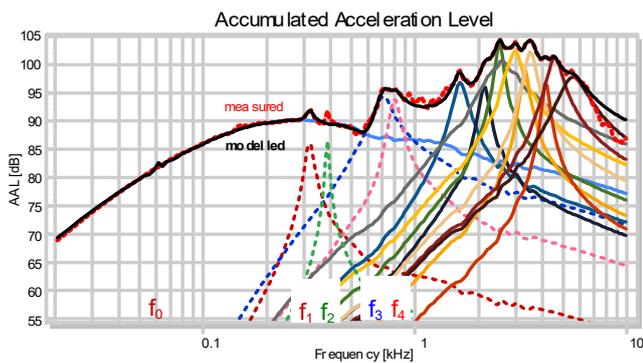

Figure 13: Contribution of the mechanical vibration modes on the radiation surface (cone, surround, dust-cap) to the measured and modelled accumulated acceleration level (AAL).

Modal Vibration

The significant values of the harmonic distortion ($EHID$) found at higher frequencies f_1, f_2, f_3, f_4 in Figure 8 can be explained by measuring the mechanical vibration by laser vibrometry and calculating the accumulated acceleration level (AAL [8]) shown as red dashed line in Figure 13. The AAL corresponds to mechanical energy of the radiation surface accessible to the laser sensor. It is comparable to the sound pressure at a defined observation point in the far field.
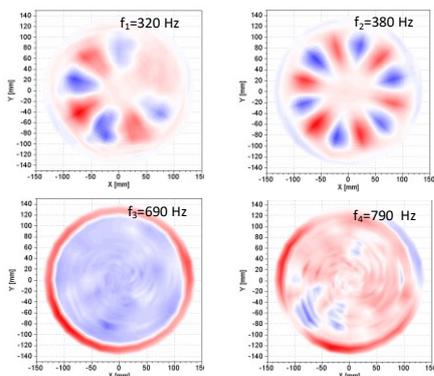

Figure 14: Vibration pattern of selected modes at natural frequencies f_1, f_2, f_3 and f_4 which generate significant 2nd-order harmonic input distortion ($EHID$) in Figure 12.

The AAL is also a convenient metric**Fehler! Verweisquelle konnte nicht gefunden werden.** [8] to perform a modal analysis. This analysis reveals the contributions of the

dominant vibration modes to the total vibration as shown in Figure 13. The AAL response of each mode reveals a 2nd-order resonance curve with a natural frequency f_n and a modal loss factor η_n. Contrary to the fundamental piston mode at f_0 the higher-order modes ($n > 0$) usually have a lower damping generating a distinct resonance peak. The higher-order modes also generate at least one nodal line in the vibration pattern (cone break-up) as shown in Figure 14 for n = 1…4. The axil-symmetrical modes at frequencies f_3 and f_4 generate an 8 dB higher AAL-value than the piston mode and a significant deformation of the surround geometry. Since the surround profile of the particular guitar speaker has a highly asymmetrical shape (few corrugation rolls), this geometrical nonlinearity generates the high level of 2nd-order distortion at the same excitation frequencies in Figure 8. The first two break-up modes at frequencies f_1 and f_2 have a circular vibration pattern on the cone as shown in Figure 14. Since those modes have 8 dB lower AAL value distributed on a much larger area than the radial modes at f_3 and f_4, the circular modes generate 2nd-order distortion that are 20 dB lower.

However, the nonlinear modal vibration in the particular guitar speaker is less critical than the motor nonlinearities $Bl(x)$ and $L(x)$ for a broad band guitar sound as used in the auralization and listening test because the spectral density of the stimulus provides a much lower excitation of the modal resonator than the sinusoidal stimulus at 25 V_{RMS}. The sonograph of the residuum reveals no symptoms of the harmonics generated by the modal resonances.

Conclusions

Recent progress in loudspeaker modeling leads to new measurements techniques that combine the physical and perceptual evaluation of the reproduced sound to understand the root cause of the distortion. Auralization techniques are the basis for systematic listening tests to investigate the audibility of signal distortions and preference of sound effect generated by design choices. Nonlinearities are not only interesting for guitar speakers but for any transducer generating more output at higher efficiency while using less resources (size, weight, energy, manufacturing effort).

References

[1] M. Zöllner, "Physik der Elektrogitarre," Regensburg 2015

[2] IEC 60268-21: Sound System Equipment – Part Acoustical (Output Based) Measurements, draft 2017

[3] IEC 60268-22: (Draft) Sound System Equipment – Electrical and Mechanical Measurements on Transducers, draft 2017

[4] W. Klippel, "Evaluation of Audio Performance Over Product Life," presented at the 142nd Convention of the Audio Eng. Soc. 2017 May 20–23, Berlin, Germany.

[5] W. Klippel, "Auralization of Signal Distortion in Audio Systems, Part 1: Generic Modeling," presented at the 51st International Conference: Loudspeakers and Headphones (August 2013)

[6] W. Klippel, "Measurement and Application of Equivalent Input Distortion," J. Audio Eng. Soc., Volume 52 Issue 9 pp. 931-947

[7] W. Klippel, "Loudspeaker Nonlinearities – Causes Parameters, Symptoms," J. Audio Eng. Soc. Vol. 54, no. 10, pp 907 – 939 (oct. 2006).

[8] W. Klippel, J. Schlechter "Distributed Mechanical Parameters of Loudspeakers, Part 1: Measurements," J. Audio Eng. Soc. Vol. 57 Issue 7/8 pp. 500-511; July 2009